Early time evolution of Freédericksz patterns generated from states of electroconvection

Denis Funfschilling* and Michael Dennin
Department of Physics and Astronomy, University of California at Irvine, Irvine, California 92697-4575, USA
(Received 28 July 2005; revised manuscript received 13 January 2006; published 11 May 2006)

We report on the early time ordering in a nematic liquid crystal subjected to a sudden change in an external ac electric field. We compare time evolution for two different initial states of electroconvection. Electroconvection is a highly driven state of a nematic liquid crystal involving convective motion of the fluid and periodic variations of the molecular alignment. By suddenly changing either the voltage or the frequency of the applied ac field, the system is brought to the same thermodynamic conditions. The time ordering of the system is characterized by the evolution of features of the power spectrum, including the average wave number, total power, and shape of the power spectrum. We observe that ordering of the system occurs faster after a sudden change in frequency than it does after a sudden change in voltage.

DOI: 10.1103/PhysRevE.73.057201 PACS number(s): 47.54.−r, 89.75.Da, 64.70.Md

Understanding systems driven far from equilibrium remains one of the outstanding challenges of contemporary physics. At the heart of the issue is the lack of any single principle that is equivalent to the minimization of free energy that is applicable in thermodynamic equilibrium [1]. A subset of this larger issue is the question of the transition between states of a system after a sudden change in an external parameter, which is known as a quench. The general question of the behavior of systems after a quench is often referred to as phase ordering or coarsening [2], as domains of the new steady state of the system order and grow.

Classically, phase ordering has been studied in the context of the transition between two *equilibrium* states. In this case, the minimization of a free energy plays a central role in understanding the ordering process [2]. More recently, transitions between *driven* states of a system have gained interest [3–12]. In this case, one considers the ordering of steady states of a driven system after the driving force has been changed. The free energy does not play a role. However, there is growing evidence that the dynamics of topological defects govern the phase ordering in both equilibrium and nonequilibrium systems [2,12,13]. One system that is useful for studying quenches in driven systems is electroconvection [10–12].

Electroconvection occurs when a nematic liquid crystal is placed between two plates and an ac electric voltage is applied perpendicular to the plates [14,15]. A nematic liquid crystal consists of long, rod-like molecules that on average are aligned along a fixed axis, which is referred to as the director. In the absence of electroconvection, the director is spatially uniform. Above a critical voltage, the director develops a periodic spatial variation, and there is an associated periodic flow, or convection rolls. The most common geometry for electroconvection is the director parallel to the glass plates initially. An interesting case exists when the director is initially perpendicular to the plates, also known as homeotropic alignment [16,17].

The dielectric anisotropy is an important parameter that is used to characterize nematic liquid crystals [15]. For an anisotropic material, such as a nematic liquid crystal, the dielectric constant is a tensor. The dielectric anisotropy is the difference between the dielectric constant for the case where the electric field and director are perpendicular and the case where they are parallel. For materials with a negative dielectric anisotropy in a homeotropic configuration, the initial transition as a function of applied voltage is the Freédericksz transition, which is followed by the transition to electroconvection [16,17]. The Freédericksz transition corresponds to the director developing a tilt relative to its initial alignment perpendicular to the plates. This state is an equilibrium state in which the angle of tilt is fixed for a given value of the voltage. However, there is a degeneracy due to the fact that the director tilt can adopt any azimuthal angle. Regions with the same azimuthal angle are usually referred to as Freédericksz domains. Once the Freédericksz transition has occurred, there is a component of the director parallel to the plates, and this configuration results in a second critical voltage at which electroconvection occurs.

The Freédericksz transition is independent of frequency; whereas the critical voltage for electroconvection is frequency dependent. This allows for exploration of two different types of quenches to the *same* equilibrium state. With different starting points, either a rapid change in frequency or voltage can bring the system to the same final frequency and voltage, and hence the same Freédericksz state. However, the system evolution to reach this final state is different. For a quench down in voltage, the average director tilt angle has to relax to the correct value. For a quench in frequency, the average tilt angle of director should already have the appropriate value. In both cases, the pattern present in the director field, charge distribution, and flow field, due to electroconvection, has to relax.

In this paper, we report on a comparison of these two quenches. We focus on the initial dynamics from the time of the quench until the point where the spatial patterns are similar. The system's evolution is characterized by a number of measures based on the power spectrum of the images. It should be noted that it is also interesting to consider the late-time evolution of the system. As the Freédericksz state is

*Present address: Department of Physics and Astronomy, University of California at Santa Barbara, Santa Barbara, California 93106-4170, USA.

an equilibrium state, the late-time evolution should be the same for both systems [2]. However, large-scale imperfections in the system complicate studies of the late-time dynamics, for which large aspects ratios are critical. Therefore, the question of the late-time behavior will be the subject of future work.

For these experiments, homeotropic cells of the nematic liquid crystal N4 were used. The liquid crystal N4 is a eutectic mixture of the two isomers of 4-methoxy-4'-*n*-butylazoxybenzene (CH_3O-C_6H_4-NON-C_6H_4-C_4H_9 and $CH_3OC_6H_4$-NNO-C_6H_4-C_4H_9). It was obtained from EM Industries (a Merck company), now EMD Chemicals Inc. [18]. The N4 was used without further purification. The method for obtaining homeotropic alignment is described in detail in Ref. [19]. Briefly, a surfactant coating is made on glass that is already treated with indium tin oxide (a transparent conductor). The surfactant coating is made using a Langmuir-Blodgett technique. A mixture of 43% of N4 and 57% arachidic acid (C20) diluted in chloroform is spread at the air-water interface, forming a monolayer that was compressed to 10 mN/m. We used C20 obtained from Sigma-Aldrich with a quoted purity of $\geqslant$99%. It was used without further purification. The pressure was held constant while the glass is coated with ten layers of the Langmuir monolayer. After the coating of the surface, the glass is baked in an oven at a temperature of 50 °C. A 25 μm mylar spacer is placed between the two glass pieces, and two opposite sides of the cell are sealed with epoxy. The cell is filled with N4 by capillary action. The two remaining sides of the cell are sealed with 5 min epoxy.

The details of the experimental apparatus are described in Ref. [20]. Essentially, there is a temperature control stage that holds the sample at a constant temperature within ±5 mK. The sample is illuminated from below and imaged from above using standard shadowgraph techniques. A pair of crossed polarizers (one below the sample and one above the sample) allow for simultaneous imaging of electroconvection patterns and of Freédericksz domains. The use of indium tin oxide (ITO) coated glass allows for the application of an ac voltage to the sample.

The general state diagram for homeotropic samples of N4 is reported in Ref. [19]. There is the expected Freédericksz transition at approximately V_{cF}=9.3 V, independent of applied frequency. The transition to electroconvection is frequency dependent. The solid black horizontal and vertical lines with triangular endpoints in Fig. 1 illustrate the two types of quenches that are reported on in this paper. The solid curve is the transition to electroconvection, and the dashed black curve is the critical voltage for the Freédericksz transition (both curves were reported in Ref. [19]). Both quenches are selected to have the same final equilibrium conditions of applied voltage and frequency within the regime where Freédericksz domains exist, but electroconvection does not. The two starting points represent different initial states for the system. The quench labeled A starts from a chaotic electroconvection state and uses a change in voltage. Physically, this means the tilt of the director must change as part of the quench. The path labeled B starts from a regular state of electroconvection and involves a change in frequency. In this case, the distance from the Freédericksz critical voltage is not changed. Therefore, the details of the initial evolution should be different.

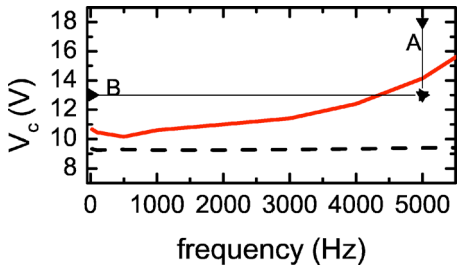

FIG. 1. (Color online) A portion of the phase diagram for homeotropic N4 as reported in Ref. [19]. The dashed curve is the critical voltage for the Freédericksz transition. The solid curve (red) is the critical voltage for the transition to electroconvection. The horizontal and vertical lines connect the starting and ending point of the two quenches.

For discussing these quenches, it is important to define a few parameters. We will use $\epsilon=(V/V_c)^2-1$ to refer to the distance from the electroconvection critical voltage (V_c) at a fixed frequency. Since all of the quenches end at a frequency f=5000 Hz and a rms voltage of V=13.0 V, the final point for the quenches is $\epsilon=-0.156$ and f=5000 Hz. The two starting points are ϵ=0.618 with f=5000 Hz and ϵ=0.490 with f=25 Hz.

To provide a framework for the two quenches, we have characterized the final state both by making quenches from below the Freédericksz critical voltage and by slowly stepping to the final state. These studies involving increasing the voltage established the existence of large-scale spatial inhomogeneities in the Freédericksz domains. Essentially the same spatial pattern is obtained either by small steps in voltage or by considering the late-time state after a large change in voltage. The spatial inhomogeneities are most likely caused by small defects in the aligning layer that result in the pinning of defects in the director organization. Because of the large-scale nature of the inhomogeneities, we do not expect them to play a significant role in the early-time evolution of the system. However, they do prevent detailed studies of the *late-time* ordering at this point, and the influence of these domains cannot be completely ruled out for the early time evolution.

For each of the quenches, we measure a series of 128 images taken 1 s apart. We characterized the images using the spatial Fourier transform of each image. We focus on the square of the modulus of the Fourier transform of each image [the power spectrum, $S(k,\theta)$, where k is the wave number of interest]. The power spectra of 20 jumps are averaged image by image to improve the statistics. There is a 15 min wait between jumps. Using $S(k,\theta)$, we measure the total power $P=\int_0^{2\pi}\int_0^{\infty}S(k,\theta)k\,dk\,d\theta=2\pi\int_0^{\infty}S(k)k\,dk$, where $S(k)$ is the azimuthal average of $S(k,\theta)$. From this measure, we observed that after a quench the total power is constant to within 10% for frequency quenches and to within 4% for voltage quenches. The average wave number,

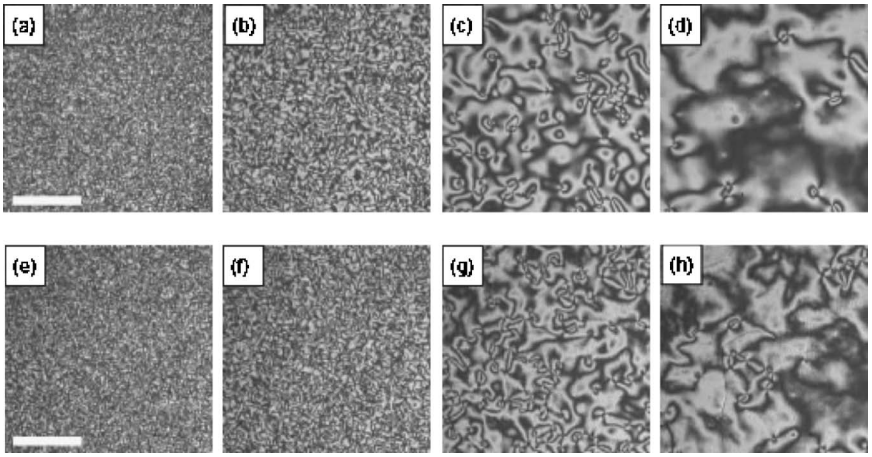

FIG. 2. Series of images for the frequency (a)–(d) and voltage (e)–(h) quenches. The white bar in the images represents 1 mm. The images are taken at 1, 4, 32, and 128 s after each quench.

$$\langle k \rangle = \frac{2\pi \int_0^\infty S(k) k^2 \, dk}{P} \tag{1}$$

is used as a measure of the typical length scale in the system, defined as $L=\langle k \rangle^{-1}$. This is used to compare the rate of growth of domains sizes for the two quenches by comparing the time dependence of the average wave number. Because we are studying the early time dynamics, it is not necessarily expected that a scaling regime will exist, but two standard methods exist for testing for scaling. First, one expects a scaling of the power spectrum of the form $S(k,t)=L^d g(kL)$, where d is the spatial dimension of the pattern. For our case, $d=2$. Second, Porod's Law [2,21] states that in the limit of large wave number ($kL \gg 1$), $S(k,t) \sim L^{-n} k^{-(d+n)}$. In this case, $d=2$ and n is the dimension of the vector order parameters that describes the system. For a nematic liquid crystal, one expects $n=2$. In this sense, Porod's law relates the behavior of the large k tail of the power spectrum to the dominant defects in the system [2].

Figure 2 presents the typical time evolution of the system after a quench in voltage. Images 2(a)–2(d) are for a frequency quench, and images 2(e)–2(h) are for a voltage quench. The images are taken at 1, 4, 32, and 128 s after the quench and illustrate the ordering that occurs. Close examination of the images reveal that after 128 s the domains are larger after a frequency quench than a voltage quench, suggesting that the ordering occurs faster after a frequency quench. This difference in ordering rate is the main result of the paper, and it is quantified in Fig. 3, which is a plot of the average wave number, $\langle k \rangle$, versus time for both quenches. The evolution of $\langle k \rangle$ confirms the faster evolution of domains after a frequency quench.

To further quantify the rate of domain growth, it is useful to fit the evolution of $\langle k \rangle$ to a power law. Despite focusing on early times, the evolution of $\langle k \rangle$ after both quenches is consistent with power law growth for the time range plotted in Fig. 3. A comparison of the exponents in the power law (-0.47 ± 0.01 for the frequency quench and -0.37 ± 0.01 for the voltage quench), confirms that the system orders faster after a frequency quench than it does after a voltage quench.

The existence of power law behavior for the evolution of the average wave number raises an interesting question: is this truly a scaling regime? Recall that the time of observation is limited by the large-scale imperfections in the cell. With just over a decade in time, it difficult to establish the existence of a scaling regime with any certainty. However, as outlined earlier, one can test for both scaling of the power spectra and scaling of the large-k tail of the power spectra. The results for scaling the azimuthally averaged power spectra are shown in Fig. 4. The results are consistent with a scaling of the power spectra, but are not conclusive. More convincing is the behavior of the spectra at large wave number. This is shown in the inset of Fig. 4 for a time 16 s after the quench. The long wave number part of the power spectra is consistent with a power law that is independent of the quench type: $S(k) \sim k^{-4}$ for large k. This result is in agreement with the expected value for ordering of a nematic liquid crystal in two dimensions [2].

Of interest for future work is the connection between the observed scaling during the early time reported here and the late-time scaling of the system. As discussed in the previous paragraph, the frequency quench does not involve significant evolution of the director tilt angle. In this case, the scaling of the average wave number was close to 1/2 (0.47 ± 0.01), the expected value for domain growth under equilibrium conditions. This suggests that the frequency quench is well described as an equilibrium process. For the voltage quench, the observed exponent was significantly smaller

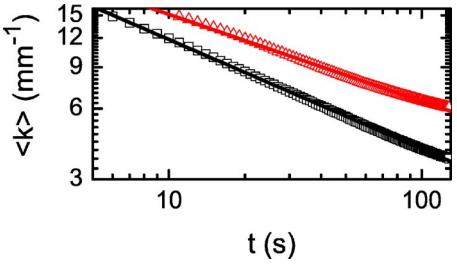

FIG. 3. (Color online) Plot of the average wave number versus time for each of the quenches. The frequency quench is represented by squares and the voltage quench is represented by triangles (red). The solid line in each case is a fit to a power law. The exponent for the frequency quench is −0.47 and for the voltage quench, it is −0.37.

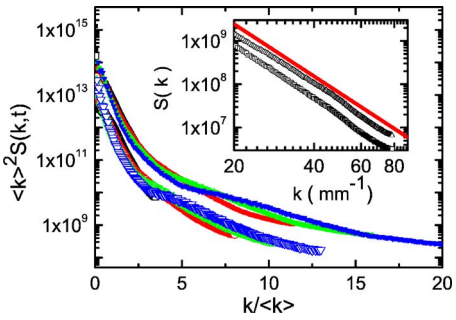

FIG. 4. (Color online) Plot of the scaled power spectra versus the average wave number for the frequency quench (solid symbols) and for the voltage quench (open symbols). The power spectra for 2, 32, 64, and 128 s after the quench is shown for each case (in black squares, red circles, green up triangles, blue down triangles, respectively). The inset shows the long time tail for 16 s after the frequency quench (squares) and the voltage quench (triangles). The solid line (red) represents k^{-4} and is provided as a guide to the eye.

(0.37 ± 0.01), and the fit to a power law is not as good for the voltage quench. (A close inspection of Fig. 3 reveals a kink in the voltage data.) Another issue with the voltage quench is the fact that different time windows of observation resulted in different effective scaling exponents that appear to converge for sufficiently long time windows. For example, for time windows of 0.1, 0.5, and 1 s, we observed exponents for the evolution of $\langle k \rangle$ of 0.28 ± 0.01, 0.35 ± 0.01, and 0.37 ± 0.01, respectively. One possible explanation for this is that the use of finite spatial windows implies that one must observe for a minimum time window before the behavior converges. In contrast, the exponent for the frequency quench was independent of the time window. A potential physical explanation for the difference in behavior of the two quenches is the fact that the voltage quench involves an evolution of the director tilt that is not present in the frequency quench. An interesting question is whether or not the behavior converges for the two processes once the director has relaxed. Such a convergence is suggested by the monotonic increase in the exponent for the voltage quench.

To summarize, we studied two quenches starting from different values of the average tilt of the director. Using the time evolution of the average wave number, the different rates of phase ordering was quantified. The frequency quench (with the same initial and final tilt) exhibited faster ordering than the voltage quench. This behavior can be understood qualitatively in terms of the different intrinsic time scales for electroconvection. The two main relaxation times are the charge relaxation time (on the order of 10^{-3} s for this system) and the director relaxation time (on the order of 1 s for this system). The voltage quench should be dominated by the director relaxation time as the system equilibrates to the equilibrium tilt angle; whereas, after a frequency quench, the director is already at the correct angle on average and the domains will order faster. The time dependence of the average wave number suggested that the growth of the domains was consistent with the existence of a scaling regime. The scaling behavior was supported by measurement of the full power spectra and the Porod tails.

ACKNOWLEDGMENT

This work was supported by NSF Grants No. DMR-9975479 and No. PRF 39070-AC9.

[1] M. C. Cross and P. C. Hohenberg, Rev. Mod. Phys. **65**, 851 (1993).
[2] A. J. Bray, Adv. Phys. **43**, 357 (1994).
[3] K. R. Elder, J. Vinals, and M. Grant, Phys. Rev. Lett. **68**, 3024 (1992).
[4] M. C. Cross and D. I. Meiron, Phys. Rev. Lett. **75**, 2152 (1995).
[5] J. J. Christensen and A. J. Bray, Phys. Rev. E **58**, 5364 (1998).
[6] D. Boyer and J. Vinals, Phys. Rev. E **65**, 046119 (2002).
[7] H. Qian and G. F. Mazenko, Phys. Rev. E **67**, 036102 (2003).
[8] H. Qian and G. F. Mazenko, Phys. Rev. E **69**, 011104 (2004).
[9] D. Boyer, Phys. Rev. E **69**, 066111 (2004).
[10] L. Purvis and M. Dennin, Phys. Rev. Lett. **86**, 5898 (2001).
[11] C. Kamaga, D. Funfschilling, and M. Dennin, Phys. Rev. E **69**, 016308 (2004).
[12] C. Kamaga, F. Ibrahim, and M. Dennin, Phys. Rev. E **69**, 066213 (2004).
[13] C. Harrison, Z. Cheng, S. Sethuraman, D. A. Huse, P. M. Chaikin, D. A. Vega, J. M. Sebastian, R. A. Register, and D. H. Adamson, Phys. Rev. E **66**, 011706 (2002).
[14] L. Kramer and W. Pesch, Annu. Rev. Fluid Mech. **27**, 515 (1995).
[15] P. G. de Gennes and J. Prost, *The Physics of Liquid Crystals* (Clarendon, Oxford, 1993).
[16] Y. Hidaka, J. H. huh, K. Jayaski, M. I. Tribelsky, and S. Kai, J. Phys. Soc. Jpn. **66**, 3329 (1997).
[17] P. Toth, A. Buka, J. Peinke, and L. Kramer, Phys. Rev. E **58**, 1983 (1998).
[18] E. Industries, Technical Documentation 2001.
[19] J. Collins, D. Funfschilling, and M. Dennin, Thin Solid Films **496**, 601 (2006).
[20] M. Dennin, Phys. Rev. E **62**, 6780 (2000).
[21] H. K. Janssen, B. Schaub, and B. Schmittmann, Z. Phys. B: Condens. Matter **73**, 539 (1989).